Applied Catalysis B: Environmental 220 (2018) 1–8

Contents lists available at ScienceDirect

Applied Catalysis B: Environmental

journal homepage: www.elsevier.com/locate/apcatb

# Dual-components modified $TiO_2$ with Pt and fluoride as deactivation-resistant photocatalyst for the degradation of volatile organic compound

Seunghyun Weon[a], Jungwon Kim[b], Wonyong Choi[a,*]

[a] Division of Environmental Science and Engineering, Pohang University of Science and Technology (POSTECH), Pohang 37673, Republic of Korea
[b] Department of Environmental Sciences and Biotechnology, Hallym University, Chuncheon, Gangwon-do 24252, Republic of Korea

ARTICLE INFO

*Keywords:*
Titanium dioxide
Surface modified $TiO_2$
Photocatalyst deactivation
Air purification
VOCs degradation

ABSTRACT

$TiO_2$ nanoparticles modified with surface platinization or/and surface fluorination (Pt/$TiO_2$, F-$TiO_2$, and F-$TiO_2$/Pt) were prepared to test their durability as an air-purifying photocatalyst. Toluene was selected as a target substrate for this test. Although Pt/$TiO_2$ showed higher photocatalytic degradation activity than bare $TiO_2$, Pt/$TiO_2$ underwent rapid deactivation during repeated degradation cycles. F-$TiO_2$ was deactivated to a lesser degree but its initial photocatalytic degradation activity was lower than bare $TiO_2$. On the other hand, F-$TiO_2$/Pt exhibited the highest photocatalytic activity and durability for toluene degradation. The surface fluorination that should replace the hydroxyl groups on $TiO_2$ surface facilitates the formation of mobile OH radicals instead of surface-bound OH radicals. The surface platinization enhances the lifetime of charge carriers and makes more holes efficiently react with adsorbed water molecules. Through the remote photocatalytic oxidation of stearic acid and coumarin coated on a glass plate that was separated from the photocatalyst film with a small air gap (50 μm), it was observed that F-$TiO_2$/Pt film generated the largest amount of mobile OH radicals that migrate through the air gap. The photocatalytic oxidation mediated by mobile OH radicals efficiently hindered the deposition of carbonaceous intermediates on the F-$TiO_2$/Pt surface and increased the mineralization efficiency of VOCs, which consequently increased the durability of photocatalyst during VOC degradation.

## 1. Introduction

The control technologies for indoor volatile organic compounds (VOCs) attract interests because modern people spend roughly 90% of their time indoors [1,2]. The indoor VOCs are emitted from various indoor materials such as furniture, decorations, and building products. The presence of VOCs can degrade the quality of the indoor environment and cause various types of health problems including headache, allergy, or nausea [3,4]. Although air filtration has been widely used for cleaning air, VOCs are adsorbed on filtration media (*e.g.,* activated carbon fiber) but not decomposed. Adsorbed VOCs can, therefore, be re-emitted from the media to the air when the adsorbents are saturated [5,6]. In this respect, photocatalytic degradation is an ideal technology for air purification because this can achieve the complete degradation of VOCs into harmless carbon dioxide and water [7–9].

Among various photocatalysts, titanium dioxide ($TiO_2$) has been widely investigated as an environmental remediation photocatalyst because of its abundance, low material cost, chemical and photochemical stability, and strong photooxidative power [10–12]. However, the deactivation of $TiO_2$ that has been frequently observed during the prolonged photocatalysis would diminish the commercial value as a practical air-purification technology [13–16]. To prevent the photocatalyst deactivation during VOC degradation, the photocatalysts modified via heterojunction with other semiconductors [17,18] and metals (Rh, Pt, and Ag) [19–21] and new photocatalyst materials were synthesized [22]. Once the photocatalyst was deactivated during air purification, it could be restored by treatment with high temperature [23], ozone [24], and irradiation in humidified air [25,26]. The deactivation of photocatalysts is often caused by the accumulation of recalcitrant intermediates and products on the surface. For example, air pollutants containing heteroatoms (Si, S, P, and N) generate inorganic products that are strongly bound to the $TiO_2$ surface to cause deactivation [27–30]. The VOC-induced deactivation of photocatalysts is caused by the strong adsorption and complexation of recalcitrant carbonaceous intermediates that are in-situ generated on the photocatalyst surface [31,32]. Since the formation of carbonaceous intermediates is often caused by an insufficient supply of $O_2$, designing open structures (*e.g.,* $TiO_2$ nanotubes) that allow facile $O_2$ diffusion was proposed as a solution for preventing photocatalyst deactivation [26,33]. To prevent the photocatalyst deactivation, either the formation of recalcitrant

* Corresponding author.
*E-mail address:* wchoi@postech.edu (W. Choi).

http://dx.doi.org/10.1016/j.apcatb.2017.08.036
Received 8 June 2017; Received in revised form 4 August 2017; Accepted 11 August 2017
Available online 14 August 2017

intermediates or the accumulation of carbonaceous deposits on the surface should be hindered.

Modifying the surface of $TiO_2$ using various methods has been extensively studied to increase the photocatalytic activity [11,12]. As a common method, loading metal nanoparticles serves as the conduction band (CB) electron sink which promotes the interfacial charge separation in the UV/$TiO_2$ system [34]. On the other hand, the surface fluorination of $TiO_2$ that substitutes the surface hydroxyl groups with fluorides ($>$Ti-OH + $F^- \rightarrow >$ Ti-F) facilitates the generation of mobile OH radicals because valence band (VB) holes react preferentially with molecularly adsorbed water instead of surface hydroxyl groups [35,36]. When $TiO_2$ was modified with both Pt nanoparticles and surface fluorides, the modified $TiO_2$ exhibited a unique property that produced $H_2$ and degraded organic compounds simultaneously in aqueous media [37]. Surface chemistry of the dual components-modified $TiO_2$ enables the production of OH radicals even in the absence of $O_2$ [38]. We particularly note that this modified $TiO_2$ efficiently generates OH radicals in $O_2$-deficient condition because this property might be utilized for inhibiting the photocatalyst deactivation that is caused by the accumulation of carbonaceous deposits during the VOC degradation.

In this study, we prepared the dual-components modified $TiO_2$ with Pt deposition and surface fluoride complexation (F-$TiO_2$/Pt) and investigated the activity and durability as an air-purifying photocatalyst during the repeated cycles of the photodegradation of gaseous toluene which was employed as a test VOC. The roles of Pt nanoparticles and surface fluorides on $TiO_2$ were discussed in relation with their synergistic effect. The photocatalytic degradation of VOCs mediated by mobile OH radical was investigated to explain the mechanism that prevents the deactivation of F-$TiO_2$/Pt.

## 2. Experimental

### 2.1. Preparation of photocatalysts

Platinum-loaded $TiO_2$ was obtained using a photodeposition method. Chloroplatinic acid ($H_2PtCl_6$) as a Pt precursor and methanol (1 M) as an electron donor were added into an aqueous suspension of commercial $TiO_2$ (P25) with an average surface area of 50 $m^2g^{-1}$ and primary particle size of 20–30 nm. The suspension was subsequently irradiated for 30 min with a 200-W mercury lamp for photodeposition. The resulting Pt/$TiO_2$ powder was collected by filtration and washed with deionized water. For VOC degradation experiments, $TiO_2$ or Pt/$TiO_2$ powder was coated on a glass substrate (2 × 2 $cm^2$) using a doctor-blade method. Photocatalyst powder was well mixed with ethanol at a concentration of 0.15 g $TiO_2$/mL. The mixed paste was spread on the glass substrate, dried under air and then heated at 200 °C for 2 h to remove residual ethanol. For the surface fluorination, aqueous solution of NaF (pH 3.5) was prepared. The coated films of $TiO_2$ and Pt/$TiO_2$ were soaked in the NaF solution for 30 min and dried under air to prepare F-$TiO_2$ and F-$TiO_2$/Pt.

### 2.2. Photocatalytic activity measurements

The VOC degradation was conducted in a closed-circulation reactor at ambient conditions [26]. The photocatalyst films of $TiO_2$, F-$TiO_2$, Pt/$TiO_2$, and F-$TiO_2$/Pt were compared for the photocatalytic degradation of toluene under the same experimental conditions. The Pyrex glass reactor (volume *ca.* 300 mL) with a quartz window (3 cm radius) and a photoacoustic gas monitor (LumaSense, INNOVA, 1412i) were connected by a Teflon tube (2 mm radius). A magnetic bar was placed inside the reactor to circulate the air in it. A 370 nm-emitting UV-LED (Luna Fiber Optic Korea, ICN14D-096) was used as a light source. The intensity of UV light flux at the surface of photocatalyst was measured to be 12 mW/$cm^2$ by a power meter (Newport, 1815-C). The photoacoustic gas monitor can measure the concentrations of toluene, carbon dioxide, and water vapor at the same time. The relative humidity (RH) was controlled at *ca.* 65% by bubbling air through a stainless steel bottle containing deionized water. Before each experiment, the reactor was flushed with high-purity air, and the photocatalyst film was pre-cleaned by UV illumination for 1 h to remove any adsorbed organic impurities. After the pre-cleaning, the concentration of toluene was adjusted by diluting the standard gas (300 ppmv toluene in Ar as a carrier gas) with high-purity air. The initial concentration of toluene was adjusted to 50 ppmv for the degradation experiments.

### 2.3. Remote photocatalytic reaction

It is proposed as a hypothesis that the photocatalytic activity mediated by mobile OH radicals is closely related with the deactivation resistance of photocatalysts. To test this hypothesis, an experimental setup that measures "remote" photocatalytic activity (*i.e.,* activity mediated by mobile OH radicals) was prepared according to a literature method [35]. In this experiment, the reaction of mobile OH radicals (generated from bare $TiO_2$, F-$TiO_2$, Pt/$TiO_2$, or F-$TiO_2$/Pt film) with *remote* stearic acids (SA) and coumarin were tested. SA-coated film was prepared by dropping SA solution ($CH_3(CH_2)_{16}COOH$, Aldrich) in methanol (12.5 mM, 80 μL) on a glass substrate (2 × 2 $cm^2$) and subsequently evaporating the methanol solvent. On the other hand, coumarin (Aldrich) was dissolved in ethanol at a concentration of 0.1 g/mL. The coumarin solution was spread on a glass substrate (2 × 2 $cm^2$) and spin-coated at a spin-rate of 3000 rpm (MIDAS system) for 30 s (repeated three times per coating). After each cycle, the coumarin-coated film was dried at 70 °C for 10 min to evaporate residual ethanol. This coumarin coating procedure was repeated five times. The SA film (or the coumarin film) and the photocatalyst film were faced to each other and held together with a small intervening air gap using a 50 μm-thick Kapton film. The photocatalyst film was prepared with a slurry of 0.075 g/mL to yield the photocatalyst film of 4–5 μm thickness to absorb incident light efficiently [39]. The sandwiched unit of the photocatalyst and SA (or coumarin) films was placed in a closed-circulation reactor and illuminated by 370 nm-emitting UV-LED.

### 2.4. Material characterizations

The High-resolution transmission electron microscopy (HR-TEM, JEOL, JEM-2200FS) with Cs correction and electron energy loss spectrum (EELS) was used for the characterization of the elemental distribution in F-$TiO_2$/Pt. X-ray photoelectron spectroscopy (XPS) (Theta Probe AR-XPS System) using the Al Kα line (1486.6 eV) as the excitation source was used to determine the surface atomic composition of F-$TiO_2$/Pt. Spectrofluorometer (HORIBA fluoromax-4) was used for analyzing the fluorescence emission (excited at 332 nm) of 7-hydroxycoumarin (with the emission centered at 450 nm) which can be generated as a result of the remote photocatalytic reaction of coumarin with mobile OH radical. Secondary ion mass spectrometry (SIMS, CAMECA, IMS 6F, $O_2+$ Gun) was used for analyzing the carbonaceous residues deposited on the photocatalyst surface (F-$TiO_2$/Pt, Pt/$TiO_2$, F-$TiO_2$, and bare $TiO_2$). Diffuse reflectance UV–vis absorption spectrophotometer (Shimadzu UV-2401PC) was used to measure the absorption spectrum of each photocatalyst.

## 3. Results and discussion

### 3.1. Characterizations of photocatalysts

The elemental distributions of Ti, O, F and Pt within the F-$TiO_2$/Pt film were measured by HR-TEM and EELS analysis (Fig. 1). Platinum nanoparticles in the size of 1–3 nm were clearly deposited on the surface of $TiO_2$ (Fig. 1a). F elemental spots were scattered on the surface of $TiO_2$ (Fig. 1e) which confirms that the surface of the F-$TiO_2$/Pt film was clearly fluorinated. The existence of platinum and fluoride on the surface of each photocatalyst film was confirmed by XPS analysis (Fig. 2).

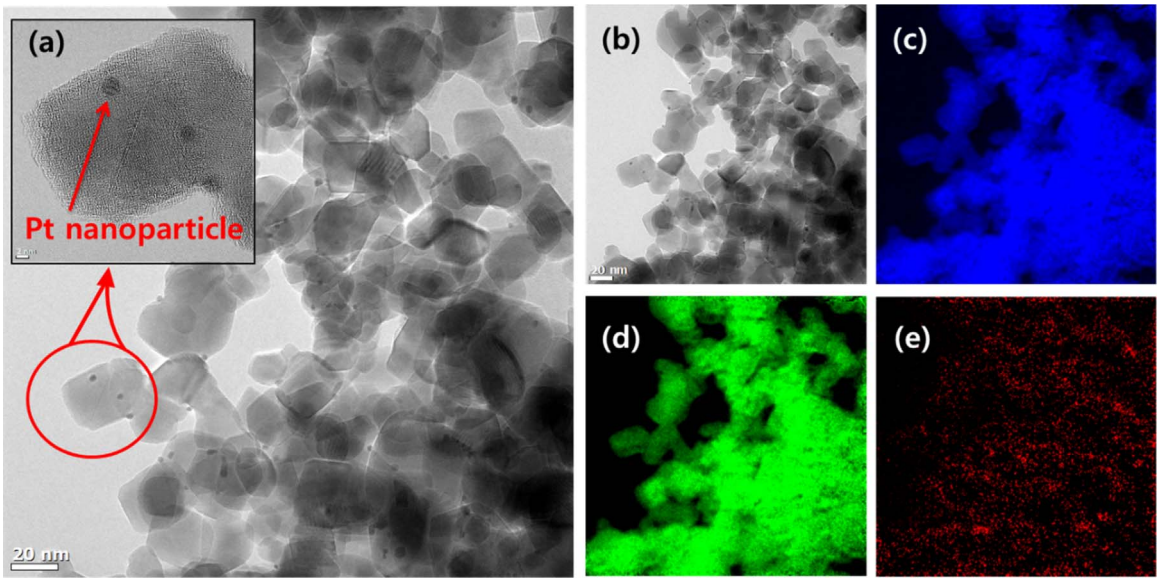


**Fig. 1.** (a) HR-TEM image of F-$TiO_2$/Pt. (b) Zero-loss filtering image and the EELS mapping of (c) Ti, (d) O, (e) F.

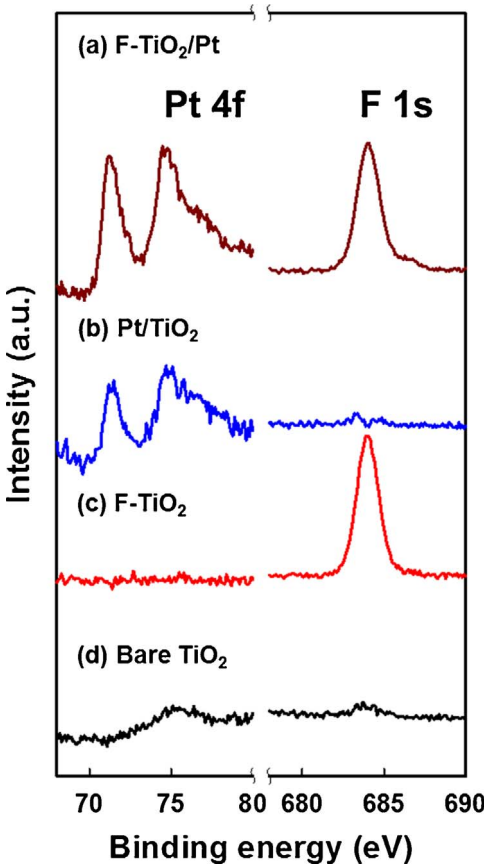


**Fig. 2.** Pt 4f and F 1s bands in XPS spectra of (a) F-$TiO_2$/Pt, (b) Pt/$TiO_2$, (c) F-$TiO_2$, and (d) bare $TiO_2$.

The peaks with binding energies of 71.28 and 74.45 eV correspond to the $4f_{7/2}$ and $4f_{5/2}$ bands of the metallic platinum deposited on the surface of $TiO_2$ [40]. The peak with binding energy of 684 eV corresponds to that of fluoride adsorbed on the $TiO_2$ surface [41]. Both Pt and F signal were observed in F-$TiO_2$/Pt, which confirms the coexistence of platinum and fluorine on the $TiO_2$ surface.

### *3.2. Photocatalytic degradation of gaseous toluene on the surface modified $TiO_2$*

The bare $TiO_2$, F-$TiO_2$, Pt/$TiO_2$, and F-$TiO_2$/Pt films were tested as an air-purifying photocatalyst for the degradation of gaseous toluene. Five successive cycles of photocatalytic degradation of toluene with an initial concentration of 50 ppmv were conducted to test the durability of each photocatalyst (Fig. 3). Each degradation cycle consisted of a dark circulation period (10 min) for adsorption equilibrium and the following irradiation period (30 min) for photocatalytic reaction. The subsequent degradation cycle resumed after the reactor was cleaned by flushing air and filled with a fresh gas containing 50 ppmv of toluene. The photocatalytic degradation activities of bare $TiO_2$, Pt/$TiO_2$, F-$TiO_2$, and F-$TiO_2$/Pt were expressed in terms of the pseudo first-order rate constants (Table 1). In the first degradation cycle, the photocatalytic activities of F-$TiO_2$/Pt and Pt/$TiO_2$ were higher than bare $TiO_2$ whereas that of F-$TiO_2$ was lower than bare $TiO_2$. It has been often reported that Pt deposits markedly increase the photocatalytic activity of $TiO_2$ for VOC degradation [42,43]. When the number of degradation cycles increased, the activity of each photocatalyst changed in different ways. In general, bare $TiO_2$ and Pt/$TiO_2$ suffered severe deactivation during the repeated cycles of photocatalytic degradation of toluene: $k(TiO_2)$ decreased to $< 5\%$ and $k(Pt/TiO_2)$ decreased to $< 15\%$ of the initial value after the fifth cycle. On the other hand, the degradation activities of F-$TiO_2$ and F-$TiO_2$/Pt decreased by less extent under the same condition: $k(F\text{-}TiO_2)$ decreased to $< 43\%$ and $k(F\text{-}TiO_2/Pt)$ decreased to $< 53\%$ of the initial value after the fifth cycle. Fig. 3 clearly shows that F-$TiO_2$/Pt is a superior air-purifying photocatalyst which maintains higher photocatalytic activity with higher durability. The activities of F-$TiO_2$/Pt samples were compared with varying the concentrations of sodium fluoride (10, 30, and 50 mM) and Pt (0.1, 0.5, and 1 wt%) to find an optimal loading as shown in Fig. 4. The activity and durability of F-$TiO_2$/Pt was optimized at 0.5 wt% Pt and 30 mM fluoride for VOC degradation and further increase in the loading of either Pt or fluoride reduced the activity on the contrary. Therefore, all the F-$TiO_2$/Pt samples tested in this study were prepared with this optimal loading of Pt and F.

It is well known that $TiO_2$ photocatalyst suffers severe deactivation during VOCs degradation. Einaga et al. reported that the toluene degradation activity of $TiO_2$ decreased by 86% within 1 h [25]. Zielinska-Jurek et al. reported that the photocatalytic degradation activity of Ag/Pt-modified $TiO_2$ decreased to 70% of the initial value after three cycle

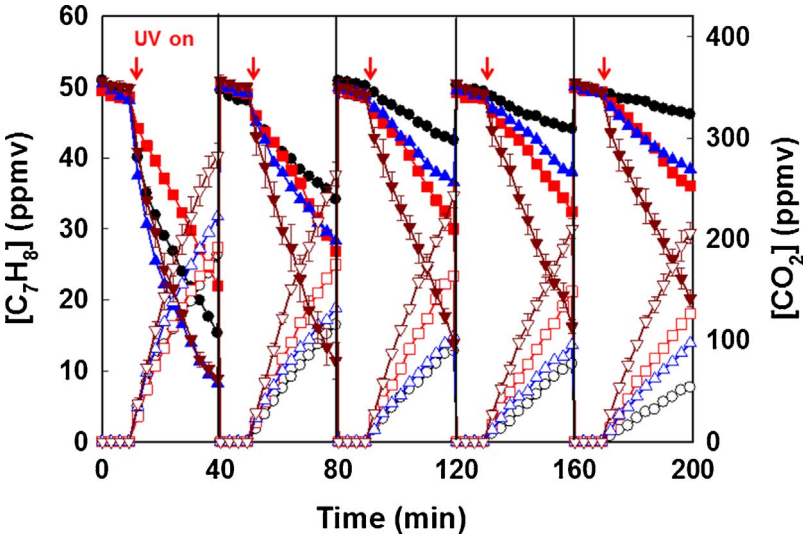


**Fig. 3.** Repeated photocatalytic degradation cycles of gaseous toluene on F-$TiO_2$/Pt (▼), Pt/$TiO_2$ (▲), F-$TiO_2$ (■), and bare $TiO_2$ (●).

**Table 1**
Change of the Toluene Degradation Rate Constants during the Successive Photocatalysis Cycles on bare $TiO_2$, Pt/$TiO_2$, F-$TiO_2$, and F-$TiO_2$/Pt.

| Cycle | Pseudo first-order rate constant ($10^{-2}$min$^{-1}$) | | | |
|---|---|---|---|---|
| | $TiO_2$ | Pt/$TiO_2$ | F-$TiO_2$ | F-$TiO_2$/Pt |
| 1 | 3.63 (±0.10) | 5.80 (±0.06) | 2.55 (±0.17) | 5.86 (±0.09) |
| 2 | 1.08 (±0.03) | 1.81 (±0.09) | 1.97 (±0.10) | 5.12 (±0.27) |
| 3 | 0.58 (±0.08) | 1.04 (±0.14) | 1.60 (±0.11) | 4.21 (±0.14) |
| 4 | 0.41 (±0.07) | 0.86 (±0.15) | 1.32 (±0.02) | 3.72 (±0.07) |
| 5 | 0.18 (±0.07) | 0.83 (±0.12) | 1.10 (±0.05) | 3.10 (±0.08) |

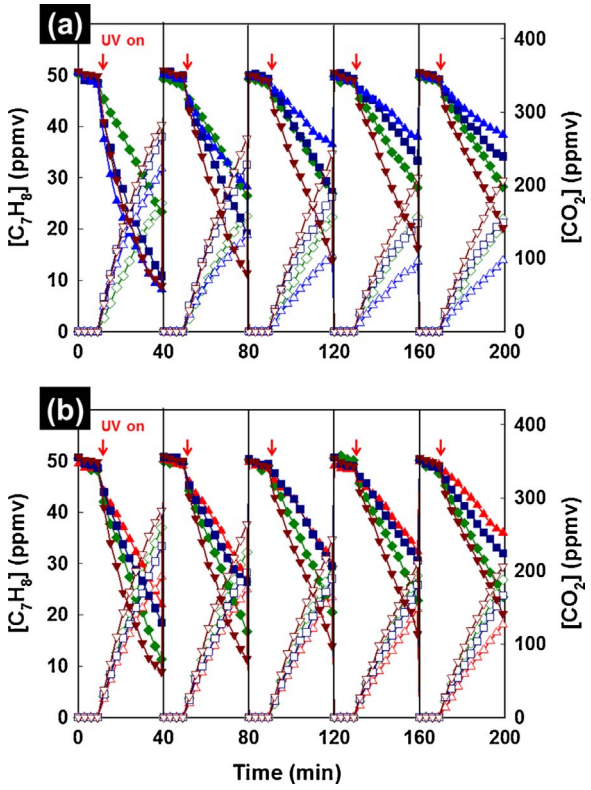


**Fig. 4.** Repeated photocatalytic degradation cycles of gaseous toluene on F-$TiO_2$/Pt with varying (a) the fluoride loading (▲: 0 mM, ■: 10 mM, ▼: 30 mM, ◆: 50 mM) and (b) Pt loading (▲: 0 wt%, ■: 0.1 wt%, ▼: 0.5 wt%, ◆: 1 wt%).

of toluene degradation [44]. In a recent study, we observed that a $TiO_2$ nanoparticulate film experienced rapid deactivation during the photocatalytic degradation of toluene whereas a $TiO_2$ nanotube film exhibited a markedly higher resistance against the deactivation [26]. The present results indicate that the simple surface modification of $TiO_2$ nanoparticulate film could have a similar effect of preventing the catalyst deactivation as in the case of the $TiO_2$ nanotubes with open structure. The degree of photocatalyst deactivation should depend on various experimental conditions (*e.g.,* mass and surface property of photocatalysts, concentration and kind of substrates, humidity level, $O_2$ concentration, light intensity, and type of photoreactor) [45,46,26] and the photocatalysts are subject to deactivation when the mineralization of VOCs occurs slowly with accumulating recalcitrant intermediates [47].

In this respect, it is important to understand how the surface modification influences the degradation and mineralization of VOCs. The effects of Pt and fluoride on the photocatalytic degradation of gaseous toluene were different. Degradation efficiency (DE = $([C_7H_8]_0 - [C_7H_8]_{30min})/[C_7H_8]_0 \times 100$) and mineralization efficiency (ME = $\triangle[CO_2]/(7 \times [C_7H_8]_0) \times 100$) of toluene in the first degradation cycle using each photocatalyst were compared in Fig. 5. Photocatalytic DE of Pt-deposited $TiO_2$ (Pt/$TiO_2$ and F-$TiO_2$/Pt) increased by 15% from that of bare $TiO_2$. The most important effect of Pt deposited on $TiO_2$ surface is to separate charge pairs through Schottky-barrier formed at the interface of $TiO_2$ surface and Pt

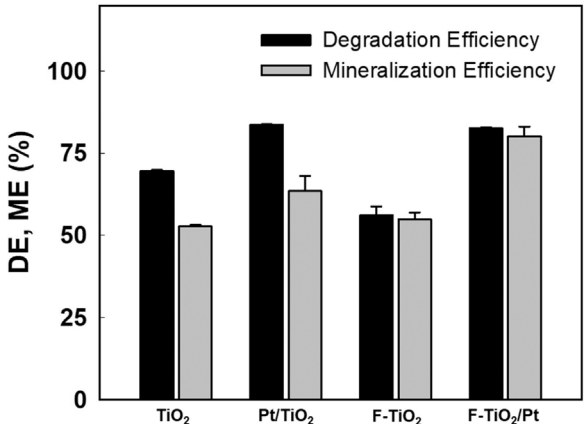


**Fig. 5.** Degradation efficiency (DE) and mineralization efficiency (ME) of photocatalytic degradation (reaction time of 30 min) of gaseous toluene on bare $TiO_2$, Pt/$TiO_2$, F-$TiO_2$, and F-$TiO_2$/Pt.

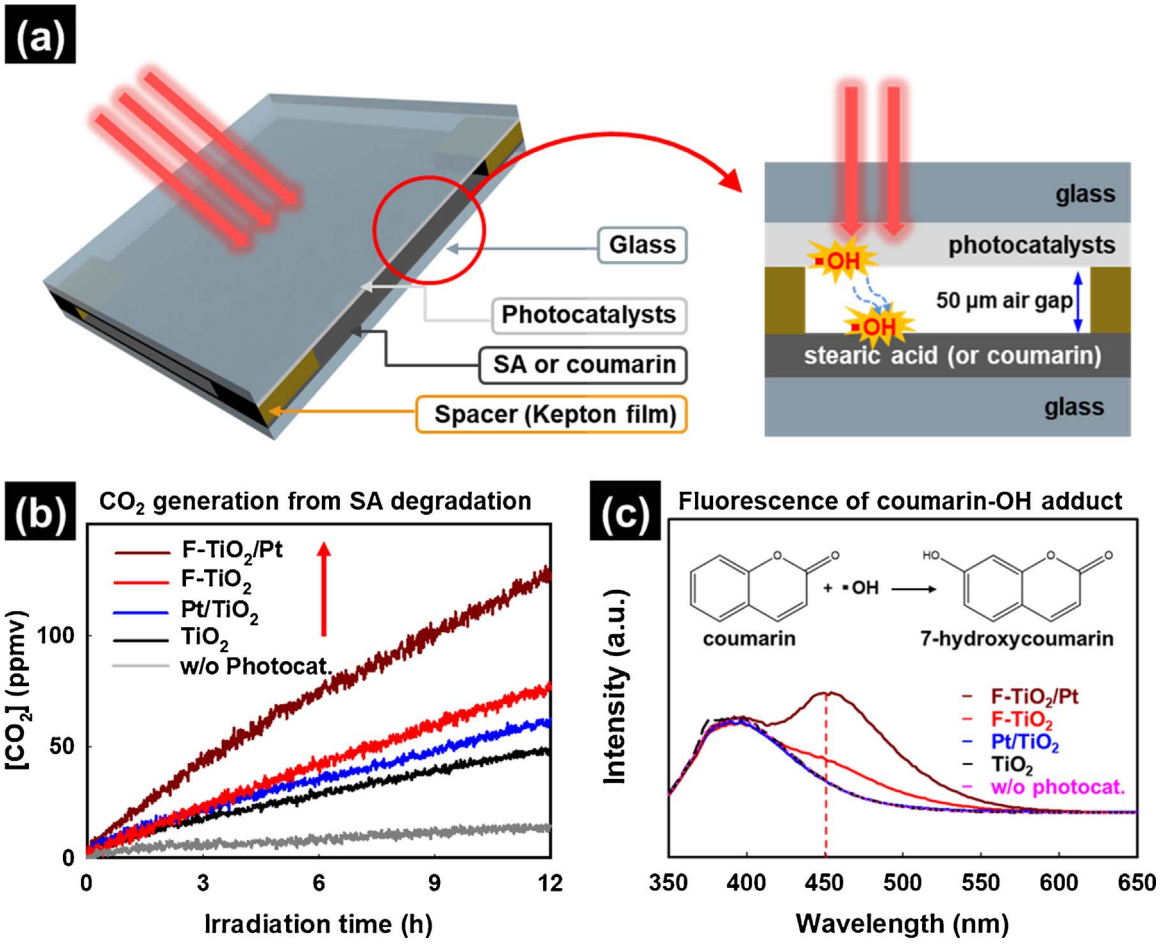


**Fig. 6.** (a) Schematic illustration of the experimental setup for the remote photocatalytic reaction of stearic acids (SA) and coumarin that are not in direct contact with the $TiO_2$ surface. (b) Remote photocatalytic degradation of SA on a glass plate that is separated from bare $TiO_2$, $Pt/TiO_2$, $F\text{-}TiO_2$, and $F\text{-}TiO_2/Pt$ film. The production of $CO_2$ was monitored to estimate the degradation of SA. (c) Remote photocatalytic oxidation of coumarin to generate the coumarin-OH adduct (7-hydroxycoumarin, 7-HC) which is generated via the reaction of coumarin with a hydroxyl radical (reaction shown in the inset). The production of 7-HC was monitored by measuring the fluorescence emission spectra ($\lambda_{em}$ = 450 nm, $\lambda_{ex}$ = 332 nm) obtained after 3-h remote photocatalytic reaction over bare $TiO_2$, $Pt/TiO_2$, $F\text{-}TiO_2$, and $F\text{-}TiO_2/Pt$ film.

nanoparticles. Charge separation process in $Pt/TiO_2$ takes place for a few picoseconds [48]. Such a rapid charge separation precedes slower interfacial charge transfer processes that lead to the formation of reactive radical species [49,50]. Therefore, efficient charge separation facilitated by the presence of Pt enables more charge carriers to be available for the generation of reactive radical species. However, it is noted that ME is lower than DE for both bare $TiO_2$ and $Pt/TiO_2$, which implies that toluene degradation intermediates are generated. On the other hand, photocatalytic ME of toluene on fluorinated $TiO_2$ films ($F\text{-}TiO_2$ and $F\text{-}TiO_2/Pt$) was very close to the corresponding DE, which means that few intermediates were generated on the surface fluorinated $TiO_2$ and the surface fluorination facilitated the mineralization process of VOCs on $TiO_2$.

The surface fluorination is a typical ligand exchange reaction between fluoride anions and hydroxyl groups on $TiO_2$ surface (Eq. (1)). The surface fluorination does not change any crystallographic structure and optical absorption of $TiO_2$ but it markedly enhances the photo-induced hydrophilicity and the adsorption of water molecules [51]. Although the surface fluorinated $TiO_2$ hinders the adsorption of organic compounds [36,52], it facilitates the generation of mobile OH radicals because the fluoride-induced depletion of surface hydroxyl groups prefer the hole transfer to the molecularly adsorbed $H_2O$ (leading to mobile OH radical) (Eq. (2)) rather than the hole transfer to the surface hydroxyl group (leading to surface-bound OH radical) (Eq. (3)). The holes that are transformed into mobile OH radicals on the fluorinated $TiO_2$ surface are less subject to the recombination with CB electrons (Eq. (4)). As a result, more holes can be utilized for oxidation reactions.

$$> \text{Ti-OH} + F^- \leftrightarrow > \text{Ti-F} + OH^- \quad (1)$$

$$> \text{Ti-F } (\textit{F-TiO}_2\ \textit{surface}) + H_2O_{ad} + {h_{vb}}^+ \rightarrow > \text{Ti-F} + H^+ + \cdot OH_{mobile} \quad (2)$$

$$> \text{Ti-OH } (\textit{bare TiO}_2\ \textit{surface}) + {h_{vb}}^+ \rightarrow > \text{Ti-OH}\cdot_{ad} \quad (3)$$

$$> \text{Ti-OH}\cdot_{ad} + {e_{cb}}^- \rightarrow > \text{Ti-OH} \quad (4)$$

The photocatalytic VOC degradation should be initiated at the active surface sites on which the oxidant radicals are generated. However, VOC degradation intermediates can be accumulated on surface sites that are distant from the active sites (*i.e.,* radical generating sites), which might induce the deposition of recalcitrant carbonaceous materials and the subsequent deactivation of the catalyst surface. In case mobile OH radicals are generated, the accumulation of recalcitrant intermediates can be significantly retarded because the oxidant radicals can migrate from the active sites to distant surface sites where the degradation intermediates might be accumulated. Such remote photocatalytic oxidation mediated by mobile OH radicals should be more efficient in preventing the catalyst deactivation caused by the in-situ deposition of carbonaceous intermediates than the photocatalytic oxidation mediated by the surface bound OH radicals. Although the surface fluorinated $TiO_2$ may retard the intrinsic degradation rate of VOCs by hindering the substrate adsorption as shown in Fig. 3 [53], the additional presence of surface platinum on $F\text{-}TiO_2/Pt$ prolongs the lifetime

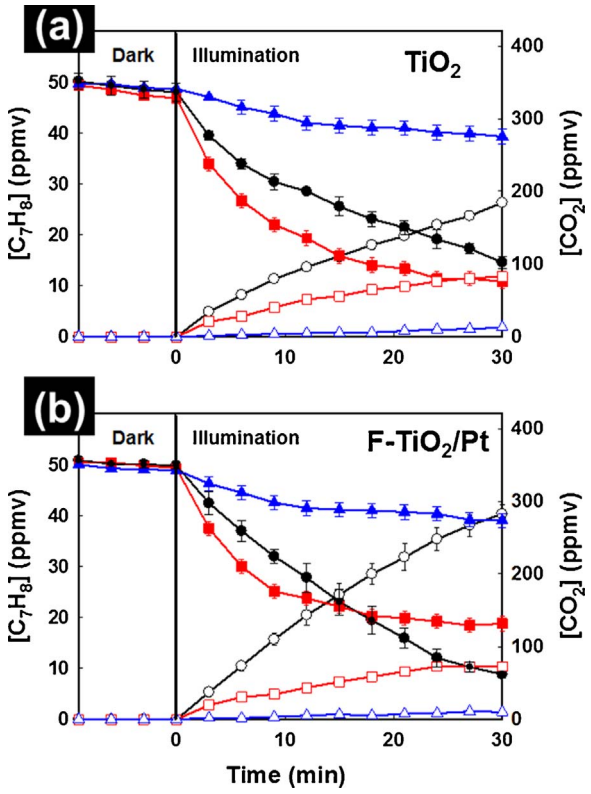


**Fig. 7.** (a) Photocatalytic degradation of gaseous toluene on (b) bare $TiO_2$ and F-$TiO_2$/Pt in ambient air (relative humidity 65%) (●), in the absence of $H_2O$ (■) and $O_2$ (▲).

of photo-generated electrons and makes more holes react with adsorbed water molecules [54]. The adsorption of degradation intermediates should be hindered on the fluorinated surface as well. As a result, the surface modified $TiO_2$ with both Pt and fluoride synergistically enhances the resistance toward the catalyst deactivation caused by the accumulation of degradation intermediates.

### 3.3. Remote photocatalytic reaction mediated by mobile OH radicals on F-$TiO_2$/Pt

The action of mobile OH radicals generated on the photocatalyst surface was indirectly confirmed by monitoring their reaction with stearic acid (SA, test substrate) that was not in direct contact with the photocatalyst surface. The experimental setup for the remote photocatalytic degradation of SA is illustrated in Fig. 6a. The SA-coated film and the photocatalyst film were faced to each other and held together with an intervening air gap of 50 μm thickness (adjusted by a spacer). The remote photocatalytic degradation was monitored by measuring the concentration of $CO_2$ generated from the degradation of SA over a distant photocatalyst film ($TiO_2$, F-$TiO_2$, Pt/$TiO_2$, and F-$TiO_2$/Pt) in ambient air (Fig. 6b). It is noted that F-$TiO_2$/Pt exhibited markedly higher $CO_2$ generation than any of bare $TiO_2$, Pt/$TiO_2$ and F-$TiO_2$. This implies that F-$TiO_2$/Pt is the most efficient in generating mobile OH radicals which should mediate the remote photocatalytic degradation.

To provide a more direct evidence that supports the generation of mobile OH radicals over F-$TiO_2$/Pt, a chemical trapping method of OH radicals was tested by employing coumarin as a chemical probe [55]. Coumarin can selectively react with OH radical to generate coumarin-OH adduct (7-hydroxycoumarin (7-HC), *see* the reaction in the inset of Fig. 6c). The remote photocatalytic oxidation of coumarin was carried out under the same experimental condition of Fig. 6b. The coumarin-coated film and the photocatalyst film were faced to each other and held together with an intervening air gap of 50 μm thickness. After 3-h UV illumination, coumarin and the reaction products (including 7-HC) were dissolved out in ethanol from the glass plate to measure the fluorescence emission ($\lambda_{em}$ = 450 nm, $\lambda_{ex}$ = 332 nm). F-$TiO_2$/Pt showed a clear sign of the production of 7-HC (coumarin-OH adduct) through the remote photocatalytic reaction while bare $TiO_2$ and Pt/$TiO_2$ showed little sign (*see* Fig. 6c). F-$TiO_2$ showed some sign of 7-HC formation, which confirms the fact that F-$TiO_2$ generates mobile OH radicals [35]. The higher production of 7-HC on F-$TiO_2$/Pt than F-$TiO_2$ in the remote photocatalysis experiment indicates that the co-presence of Pt and F species on $TiO_2$ works synergically to generate a larger number of OH radicals.

The average lifetime of OH radical ($\tau_{OH}$) in an ambient atmospheric condition is around 0.01–1 s [56], which is affected by the concentration of reactive gas components such as $O_3$, VOCs, and $NO_x$ [57]. Since the present remote photocatalysis experiments with different photocatalysts were carried out under the same experimental condition, the lifetime of mobile OH radicals in the gas phase should be the same regardless of the kind of photocatalyst. The typical gas diffusion coefficients at ambient atmospheric condition range in 0.1–0.2 $cm^2\ s^{-1}$. As a result, mobile OH radicals, if they are present, could easily migrate through the gap distance of 50 μm to reach remote SA molecules according to a rough estimation of the diffusion length (L): $L = [(0.1\ cm^2\ s^{-1})*(0.01\ s)]^{0.5} = 0.32$ mm for $\tau_{OH} = 0.01$ s or L = 0.32 cm for $\tau_{OH} = 1$ s, both of which are far greater than 50 μm. Therefore, once OH radicals are desorbed from the irradiated photocatalyst surface into the gas phase, they are able to diffuse through the ambient air through the distance of 1 mm or so and the production of such mobile OH radicals are highly enhanced when both Pt and F species are loaded on the surface of $TiO_2$ as we demonstrated in Fig. 6. The mobile OH radicals should be more efficient in degrading and mineralizing the recalcitrant substrates and intermediates, which should be related with why F-$TiO_2$/Pt is more resistant against the deactivation.

To investigate the different mechanistic behaviors of bare $TiO_2$ and F-$TiO_2$/Pt, the effects of $O_2$ and water vapor on the photocatalytic degradation activities are compared in Fig. 7. The absence of $O_2$ significantly hindered the photocatalytic degradation for both bare $TiO_2$ and F-$TiO_2$/Pt since there were no efficient acceptors of CB electrons and, therefore, the production of $CO_2$ was almost negligible. On the other hand, the absence of $H_2O$ vapor enhanced the initial degradation rate for both bare $TiO_2$ and F-$TiO_2$/Pt but suppressed the production of $CO_2$ on the contrary. Such behavior can be explained by two competing effects that (1) $H_2O$ molecules are adsorbed on $TiO_2$ surface to block the adsorption site of toluene molecules and (2) $H_2O$ molecules are the precursor of OH radicals. In the lack of adsorbed $H_2O$ molecules, toluene molecules can be more easily accessible to the active surface sites, which enhances the initial degradation rate. However, the lack of adsorbed $H_2O$ molecules should lead to the hindered production of surface OH radicals, which subsequently reduce the mineralization efficiency. As a result, it has been often reported that there is an optimal concentration of $H_2O$ vapor to maximize the VOC degradation rate [45]. It is interesting to note that the removal rate of toluene on F-$TiO_2$/Pt was rapidly decelerated in the absence of water vapor after 10 min irradiation. This indicates that molecularly adsorbed $H_2O$ molecules on F-$TiO_2$/Pt are rapidly depleted in the absence of water vapor. This is an indirect evidence that holes preferentially react with surface-adsorbed $H_2O$ molecules on the fluorinated $TiO_2$ surface (Eq. (2)).

The photocatalytic degradation mechanisms occurring on bare $TiO_2$ and F-$TiO_2$/Pt are illustrated in Scheme 1. On bare $TiO_2$, VB hole primarily reacts with surface hydroxyl group to generate surface-bound OH radical (Eq. (3)), but the holes trapped at the surface hydroxyl groups can be readily recombined with a CB electron (Eq. (4)) [58], which limits the reactivity of the surface-bound OH radical. However, when fluorides are adsorbed on $TiO_2$ with replacing the surface OH groups, the reduced density of surface hydroxyl groups enhances the portion of holes reacting with adsorbed water molecules (generating mobile OH radicals) (Eq. (2)) with decreasing the portion of holes reacting with the surface hydroxyl groups (generating surface bound OH

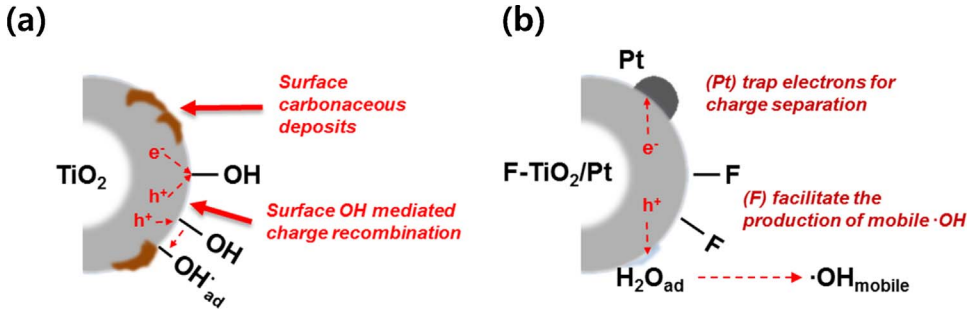


**Scheme 1.** Schematic illustration of the photocatalytic reaction processes occurring on the surface of (a) bare $TiO_2$ and (b) F-$TiO_2$/Pt.

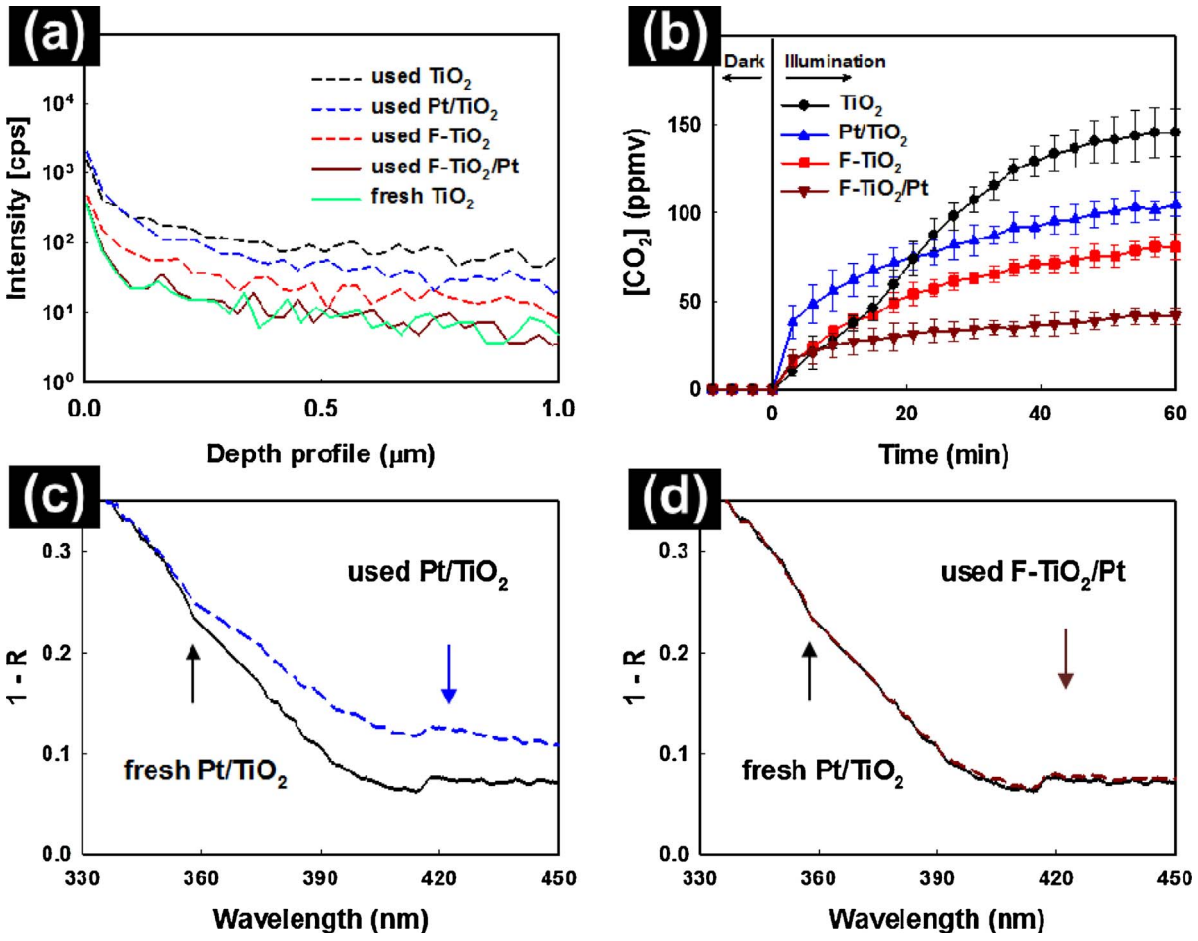


**Fig. 8.** (a) Carbon signals from dynamic SIMS depth profiling for the used samples of bare $TiO_2$, Pt/$TiO_2$, F-$TiO_2$, F-$TiO_2$/Pt (after five cycles of photocatalytic degradation of toluene) and fresh $TiO_2$. (b) Time profiles of $CO_2$ generation (in fresh air without toluene) from the photocatalytic degradation of carbonaceous material *in-situ* formed on the used samples of bare $TiO_2$, Pt/$TiO_2$, F-$TiO_2$, and F-$TiO_2$/Pt. (c) Diffuse reflectance UV–vis absorption spectra of fresh Pt/$TiO_2$ and used Pt/$TiO_2$. (d) Diffuse reflectance UV–vis absorption spectra of fresh F-$TiO_2$/Pt and used F-$TiO_2$/Pt.

radicals) (Eq. (3)). The enhanced photoinduced hydrophilicity of F-$TiO_2$ should facilitates the hole reaction with adsorbed water molecules [51]. On the other hand, the role of Pt deposits is to trap electrons while holes react with adsorbed water molecules. Consequently, when both Pt and F species are present on $TiO_2$, a larger number of mobile OH radicals should be generated on the surface of F-$TiO_2$/Pt, which should enhance the photocatalytic activity and the resistance against the catalyst deactivation during VOC degradation.

### 3.4. Carbonaceous deposits formed on photocatalyst surface

During the photocatalytic degradation of gaseous toluene, the addition of OH radical on the aromatic ring of toluene leads to the formation of cresols [59]. Benzyl alcohol, benzaldehyde, and benzoic acid are also generated as by-products of toluene degradation [59,60]. These hydrophilic intermediates are more strongly adsorbed on $TiO_2$ surface than the parent toluene molecules, and some of them can be further transformed into condensed products (with higher molecular weight) unless they are rapidly mineralized to $CO_2$ [61]. Hydrophilic aromatic intermediates (*e.g.,* benzoic acid) adsorbed on the surface may serve as an external recombination site of charge carriers to hinder further oxidation of intermediates [18,62]. The accumulation of recalcitrant carbonaceous intermediates on the $TiO_2$ surface should block the active sites and consequently hinder the access of substrate molecules to the active sites, which should be the main cause for the photocatalyst deactivation.

The photocatalyst films (bare $TiO_2$, Pt/$TiO_2$, F-$TiO_2$, and F-$TiO_2$/Pt) that had been used in five successive cycles of photocatalytic

degradation of toluene were analysed by dynamic SIMS depth profiling to measure the amount of carbonaceous deposits on each photocatalyst surface (Fig. 8a). The carbon signal intensities of the deactivated $TiO_2$ and $Pt/TiO_2$ were clearly higher compared with fresh $TiO_2$, which indicates that the surface of $TiO_2$ and $Pt/TiO_2$ was covered with carbonaceous material after five cycles of photocatalytic degradation. The carbon signal intensities were higher in the surface region (< 0.5 μm) and rapidly decreased with the depth because most carbonaceous materials should be present on the surface region. On the other hand, the carbon signal intensities of the deactivated F-$TiO_2$/Pt showed little difference from those of fresh $TiO_2$, which indicates the lack of carbonaceous deposits on the surface of F-$TiO_2$/Pt even after five cycles of toluene degradation. To regenerate the clean surface, the above deactivated photocatalyst films ($TiO_2$, $Pt/TiO_2$, F-$TiO_2$, and F-$TiO_2$/Pt) were illuminated under UV irradiation in clean air (without any toluene), which removed the carbonaceous material photocatalytically [26]. The evolution of $CO_2$ from the photocatalytic degradation of in-situ formed carbonaceous deposits was measured as a function of UV irradiation time (Fig. 8b), which can be used as an indirect method of estimating the amount of deposited carbon material. The evolution of $CO_2$ rapidly increased in the initial stage and was saturated after 1 h of UV irradiation, which means most carbonaceous deposits on the surface of photocatalyst were completely mineralized to $CO_2$ within 1 h UV irradiation. The final concentration of evolved $CO_2$ (*a measure of oxidized carbons*) was in the order of $TiO_2$ > $Pt/TiO_2$ > F-$TiO_2$ > F-$TiO_2$/Pt, which reconfirms that F-$TiO_2$/Pt accumulated the lowest amount of carbon deposits after the five cycles of photocatalysis. This is also consistent with the analysis of SIMS depth profiling. Once the $TiO_2$ surface was deactivated, the color of $TiO_2$ film changed from white to light brown because of the accumulation of carbonaceous deposits, which could be also checked by the change of the spectral reflectance. The diffuse reflectance spectrum of the used $Pt/TiO_2$ showed an elevated background in the visible region (Fig. 8c) whereas that of the used F-$TiO_2$/Pt showed little difference from the fresh sample (Fig. 8d). This also confirms that F-$TiO_2$/Pt prevented the accumulation of carbonaceous deposits during the photocatalytic degradation of toluene.

## 4. Conclusions

The deactivation of photocatalysts is the main obstacle that prevents the commercialization of air-purifying photocatalysts. This study introduced dual-components modified $TiO_2$ with surface fluorination and platinization for preventing the deactivation of $TiO_2$ photocatalyst. This study found that the modified $TiO_2$ has a notable deactivation-resistant property during the photocatalytic degradation of toluene. To prevent photocatalysts from being deactivated during VOC degradation, it is important to hinder either the formation of recalcitrant intermediates or the accumulation of carbonaceous deposits on the surface of photocatalyst. The surface fluorination enhances the generation of mobile OH radicals while it should hinder the adsorption of VOCs and their degradation intermediates. On the other hand, the surface Pt increases the lifetime of charge carriers with making more holes react with adsorbed water molecules to generate mobile OH radicals. As a result, by combining both surface fluorination and platinization on $TiO_2$, a larger number of mobile OH radicals could be generated on F-$TiO_2$/Pt, which exhibited a highly enhanced activity of remote photocatalytic oxidation (mediated by mobile OH radicals) and a high resistance against the catalyst surface deactivation. The dual-components modified $TiO_2$ (F-$TiO_2$/Pt) achieved the higher DE and ME of VOCs as well as higher durability in comparison with other photocatalysts ($TiO_2$, F-$TiO_2$, and $Pt/TiO_2$).

## Acknowledgements

This research was financially supported by Global Research Laboratory (GRL) Program (No. NRF-2014K1A1A2041044) and Basic Science Research Program (NRF-2017R1A2B2008952) funded by Korea NRF and a project funded by Samsung Electronics.

## References

[1] W. Nazaroff, A. Goldstein, Indoor Air 25 (2015) 357.
[2] R. Habre, B. Coull, E. Moshier, J. Godbold, A. Grunin, A. Nath, W. Castro, N. Schachter, N. Rohr, A. Kattan, M. Kattan, J. Spengler, P. Koutrakis, J. Expo. Sci. Environ. Epidemiol. 24 (2014) 269.
[3] J. Chin, C. Godwin, E. Parker, T. Robins, T. Lewis, P. Harbin, S. Batterman, Indoor Air 24 (2014) 403.
[4] A. Chaudhary, S. Hellweg, Environ. Sci. Technol. 48 (2014) 14607.
[5] F. Khan, A. Ghoshal, J. Loss Prev. Process Ind. 13 (2000) 527.
[6] M. Sidheswaran, H. Destaillats, D. Sullivan, S. Cohn, J. Larsen, W. Fisk, Build. Environ. 47 (2012) 357.
[7] S. Wang, H. Ang, M. Tade, Environ. Int. 33 (2007) 694.
[8] Y. Huang, S. Ho, Y. Lu, R. Niu, L. Xu, J. Cao, S. Lee, Molecules 21 (2016) 56.
[9] H. Kim, H. Kim, S. Weon, G. Moon, J. Kim, W. Choi, ACS Catal. 6 (2016) 8350.
[10] M.R. Hoffmann, S.T. Martin, W. Choi, D.W. Bahnemann, Chem. Rev. 95 (1995) 69.
[11] H. Park, Y. Park, W. Kim, W. Choi, J. Photochem. Photobiol. C 15 (2013) 1–20.
[12] H. Park, H. Kim, G. Moon, W. Choi, Energy Environ. Sci. 9 (2016) 411.
[13] J. Mo, Y. Zhang, Q. Xu, J. Lamson, R. Zhao, Atmos. Environ. 43 (2009) 2229.
[14] J. Carneiro, J.A. Moulijn, G. Mul, J. Catal. 273 (2010) 199.
[15] B.I. Stefanov, G.A. Niklasson, C. Granqvist, L. Osterlund, J. Catal. 335 (2016) 187.
[16] A. Mamaghani, F. Haghighat, C. Lee, Appl. Catal. B: Environ. 203 (2017) 247.
[17] J. Wang, H. Ruan, W. Li, D. Li, Y. Hu, J. Chen, Y. Shao, Y. Zheng, J. Phys. Chem. C 116 (2012) 13935.
[18] M. Hernandez-Alonso, I. Tejedor-Tejedorb, J. Coronadoc, M. Anderson, Appl. Catal. B: Environ. 101 (2011) 283.
[19] H. Einaga, T. Ibusuki, S. Futamura, Environ. Sci. Technol. 38 (2004) 285.
[20] L. Zhang, J. Yu, Catal. Commun. 6 (2005) 684.
[21] Z. Wu, Z. Sheng, Y. Liu, H. Wang, J. Mo, J. Hazard. Mater. 185 (2011) 1053.
[22] T. Yan, J. Long, X. Shi, D. Wang, Z. Li, X. Wang, Environ. Sci. Technol. 44 (2010) 1380.
[23] S. Sun, J. Ding, J. Bao, C. Gao, Z. Qi, X. Yang, B. He, C. Li, Appl. Surf. Sci. 258 (2012) 5031.
[24] M. Krichevskaya, S. Presi, A. Moiseev, N. Pronina, J. Deubener, Catal. Today 280 (2017) 93.
[25] H. Einaga, S. Futamura, T. Ibusuki, Appl. Catal. B: Environ. 38 (2002) 215.
[26] S. Weon, W. Choi, Environ. Sci. Technol. 50 (2016) 2556.
[27] J. Peral, D. Ollis, J. Mol. Catal. A 115 (1997) 347.
[28] D. Kozlov, A. Vorontosov, P. Smirniotis, E. Savinov, Appl. Catal. B: Environ. 42 (2003) 77.
[29] M. Chemweno, L. Cernohlavek, W. Jacoby, J. Air Waste Manage. Assoc. 58 (2008) 12.
[30] R. Portela, R. Tessinari, S. Suarez, S. Rasmussen, M. Hernandez-Alonso, M. Canela, P. Avila, B. Sanchez, Environ. Sci. Technol. 46 (2012) 5040.
[31] N. Abbas, M. Hussain, N. Russo, G. Saracco, Chem. Eng. J. 175 (2011) 330.
[32] F. Thevenet, C. Guillard, A. Rousseau, Chem. Eng. J. 244 (2014) 50.
[33] S. Weon, J. Choi, T. Park, W. Choi, Appl. Catal. B: Environ. 205 (2017) 386.
[34] S. Hamid, I. Ivanova, T. Jeon, R. Dillert, W. Choi, D. Bahnemann, J. Catal. 349 (2017) 128.
[35] J. Park, W. Choi, Langmuir 20 (2004) 11523.
[36] H. Park, W. Choi, J. Phys. Chem. B 108 (2004) 4086.
[37] J. Kim, D. Monllor-Satoca, W. Choi, Energy Environ. Sci. 5 (2012) 7647.
[38] J. Kim, J. Lee, W. Choi, Chem. Commun. 5 (2008) 756.
[39] E. Carbonell, F. Ramiro-Manzano, L. Rodriguez, A. Corma, M. Francisco, H. Garcia, Photochem. Photobiol. Sci. 7 (2008) 931.
[40] M. Martin, E. Lee, H. Kim, W. Yoon, Y. Kwon, J. Mater. Chem. A 3 (2015) 17154.
[41] J. Yu, Q. Xiang, J. Run, S. Mann, CrystEngComm 12 (2010) 872.
[42] T. Sano, N. Negishi, K. Uchino, J. Tanaka, S. Matsuzawa, K. Takeuchi, J. Photochem. Photobiol. A-Chem. 160 (2003) 93.
[43] S. Lee, J. Scott, K. Chiang, R. Amal, J. Nanopart. Res. 11 (2009) 209.
[44] A. Zielinska-Jurek, A. Zaleska, Catal. Today 230 (2014) 104.
[45] J. Mo, Y. Zhang, Q. Xu, Appl. Catal. B: Environ. 132–133 (2013) 212.
[46] M. Le Bechec, N. Kinadjian, D. Ollis, R. Backov, S. Lacombe, Appl. Catal. B 179 (2015) 78.
[47] S. Hay, T. Obee, Z. Luo, T. Jiang, Y. Meng, J. He, S. Murphy, S. Suib, Molecules 20 (2015) 1319.
[48] H. Furube, T. Asahi, H. Masuhara, H. Yamashita, M. Anpo, Chem. Phys. Lett. 336 (2001) 424.
[49] W. Teoh, L. Madler, R. Amal, J. Catal. 251 (2007) 271.
[50] B. Fraters, R. Amrollahi, G. Mul, J. Catal. 324 (2015) 119.
[51] J. Tang, H. Quan, J. Ye, Chem. Mater. 19 (2007) 116.
[52] H. Kim, W. Choi, Appl. Catal. B: Environ. 69 (2007) 127.
[53] M. Lewandowski, D. Ollis, J. Catal. 217 (2003) 38.
[54] S. Kuwahara, K. Katayama, Phys. Chem. Chem. Phys. 18 (2016) 25271.
[55] K. Ishibashi, A. Fujishima, T. Watanabe, K. Hashimoto, Electrochem. Commun. 2 (2000) 207.
[56] E. Gomez Alvarez, D. Amedro, A. Charbel, S. Gilgorovski, C. Schoemaecker, C. Fittschen, J. Doussin, H. Wortham, Proc. Natl. Acad. Sci. U. S. A. 110 (2013) 13294.
[57] S. Gligorovski, R. Strekowski, S. Barbati, D. Vione, Chem. Rev. 115 (2015) 13051.
[58] J. Ryu, W. Kim, J. Kim, J. Ju, J. Kim, Catal. Today 282 (2017) 24.
[59] J. Mo, Y. Zhang, Q. Zu, Y. Zhu, J. Lamson, R. Zhao, Appl. Catal. B: Environ. 89 (2009) 570.
[60] I. Dhada, M. Sharma, P. Nagar, J. Hazard. Mater. 316 (2016) 1.
[61] M. Sleiman, P. Conchon, C. Ferronato, J. Chovelon, Appl. Catal. B: Environ. 86 (2009) 159.
[62] N. Martsinovich, D. Jones, A. Troisi, J. Phys. Chem. C 114 (2010) 22659.